Original Article

JCBFM

Journal of Cerebral Blood Flow & Metabolism
2017, Vol. 37(6) 2076–2083

DOI: 10.1177/0271678X16660985
journals.sagepub.com/home/jcbfm
SAGE

MRI of cerebral micro-vascular flow patterns: A multi-direction diffusion-weighted ASL approach

JA Wells[1,2], DL Thomas[3,4], T Saga[1], J Kershaw[1] and I Aoki[1]

Abstract

The study and clinical assessment of brain disease is currently hindered by a lack of non-invasive methods for the detailed and accurate evaluation of cerebral vascular pathology. Angiography can detect aberrant flow in larger feeding arteries/arterioles but cannot resolve the micro-vascular network. Small vessels are a key site of vascular pathology that can lead to haemorrhage and infarction, which may in turn trigger or exacerbate neurodegenerative processes. In this study, we describe a method to investigate microvascular flow anisotropy using a hybrid arterial spin labelling and multi-direction diffusion-weighted MRI sequence. We present evidence that the technique is sensitive to the mean/predominant direction of microvascular flow in localised regions of the rat cortex. The data provide proof of principle for a novel and non-invasive imaging tool to investigate cerebral micro-vascular flow patterns in healthy and disease states.

Keywords

Arterial spin labelling, diffusion imaging, micro-vascular, perfusion, magnetic resonance imaging

Received 23 March 2016; Revised 17 June 2016; Accepted 23 June 2016

Introduction

Changes in cerebral perfusion are a prevailing feature of acute and chronic brain disorders. Wide ranging evidence has prompted several theories that posit micro-vascular abnormalities as pivotal in the aetiology of neurodegenerative disease.[1–3] Detailed characterisation of micro-vascular flow patterns in humans and in animal models of disease may help elucidate the precise role of aberrant perfusion in brain pathology, informing future therapeutic strategies for conditions such as Alzheimer's disease and vascular dementia. Optical microscopy and photoacoustic techniques can image the local architecture of superficial cerebral microcirculation, but are invasive and cannot be applied clinically. Therefore new, non-invasive and translatable techniques that are sensitive to patterns of micro-vascular flow across the whole brain may be highly useful in the study and diagnosis of brain pathology in both clinical and research settings.

Diffusion-weighted imaging (DWI) is an established MRI technique that generates contrast by sensitising measurements to the random molecular motion of water.[4] Diffusion sensitising gradients (or motion probing gradients (MPGs)) can be applied in multiple directions to capture the directional bias of tissue diffusion.[5] In the brain, regionally dependent anisotropy of the diffusion-weighted signal is observed due to the ordered nature of the underlying tissue microstructure. A notable example is white matter tracts, where the estimated directionality of tissue diffusion aligns with the dominant axonal orientation within a voxel, reflecting the relatively free diffusion of water along the axon and restricted or hindered diffusion perpendicular to it.[6] The intra-voxel incoherent motion (IVIM) method employs MPGs to detect the high

[1]National Institute of Radiological Sciences (NIRS), National Institute for Quantum and Radiological Science and Technology (QST), Chiba, Japan
[2]UCL Centre for Advanced Biomedical Imaging, University College London, London, UK
[3]Department of Brain Repair and Rehabilitation, UCL Institute of Neurology, London, UK
[4]Leonard Wolfson Experimental Neurology Centre, UCL Institute of Neurology, London, UK

Corresponding author:
JA Wells, UCL Centre for Advanced Biomedical Imaging, University College London, 72 Huntley Street, London WC1E 6DD, UK.
Email: jack.wells@ucl.ac.uk

pseudo-diffusion coefficient (PDC) that is attributed to the vascular component of the tissue.[7,8] IVIM metrics have been shown to correlate with changes in cerebral perfusion, with greater PDCs associated with increased flow.[9]

The dominant orientation of cerebral micro-vascular flow patterns may be detectible by combining the principles underlying IVIM and multi-direction DWI, i.e. by taking IVIM measurements with MPGs applied in multiple directions. This hybrid approach might be employed to map the architecture of the microcirculation in an analogous way to traditional multi-direction DWI of white matter fibre orientation. Indeed, previous studies have performed simulations and measurements in phantoms and in an isolated perfused heart in support of this concept.[10,11] Further experiments have provided evidence for microvascular flow anisotropy in vivo, in skeletal muscle and in the kidney, using this combined approach.[10,12] Yet, to date, no empirical evidence exists to support meaningful application of this idea to the brain. To address this challenge, here we propose a new approach which employs arterial spin labelling (ASL) with short inflow times (TI) to target the micro-vascular MRI signal. We combine ASL with multi-direction MPGs to investigate the dominant direction of micro-vascular perfusion in the rat brain. We present evidence that this method can detect regionally specific directionality of cerebral micro-vascular flow orientation. These data provide proof of principle for a novel, non-invasive, quantitative and directly translatable method to image cerebral arterial microvascular flow patterns using MRI.

Two hypotheses to support the proof of principle of the methodology

A striking feature of the rodent cerebral vasculature is the morphology of the penetrating arterioles in the cortex.[13,14] When viewed in the coronal plane, these vessels are orientated perpendicular to the cortical surface[15] and align radially inwards, in parallel with their local neighbours (illustrated schematically in Figure 4(a)). We examined two hypotheses to provide evidence that the hybrid ASL/multi-direction DWI protocol used in this study can yield biologically meaningful information that accurately reflects the dominant micro-vascular orientation within a voxel. The two hypotheses were based on the known morphometry of the penetrating arterioles in a coronal slice of the cortex, together with the temporal dynamics of blood delivery and exchange, and are summarised as follows:

1. The dominant directionality of the ASL diffusion-weighted signal will follow the orientation of the penetrating arterioles (i.e. radially inwards) from the medial to the lateral section of the cortex within the coronal slice.
2. The extent of the directionality of the ASL diffusion-weighted signal from the medial to lateral potion of the cortex will decrease at greater TI, as the ASL signal shifts to the more isotropic capillaries from the 'directionally ordered' penetrating arterioles.

Methods

MRI data acquisition

The animal use and experimental protocols were approved through the Institutional Animal Care and Use Committee of the National Institute of Radiological Sciences (NIRS; Chiba, Japan), and conducted in accordance with the institutional guidelines set for animal experiments by NIRS and following the ARRIVE guidelines (Animal Research: Reporting of In Vivo Experiments). Five male Sprague Dawley rats (267 ± 22 g, $n = 5$) were anaesthetised and maintained on 2% isoflurane in a 3/1 mixture of air/O_2 during imaging. Animals were free breathing and isoflurane concentration was gradually reduced to ~1.7% during the imaging period to maintain respiration rate between 60 and 90 bpm. Rats were secured with ear bars and a nose cone and were positioned supine inside the MRI scanner bore. Respiration and temperature were monitored using a pressure sensitive pad and rectal probe. Rectal temperature was maintained between 36 and 37°C using an electrically heated bed and hot air fan.

Images were acquired using a preclinical 7T MRI scanner (40-cm bore diameter, Biospec AVANCE-I system, Bruker Biospin, Ettlingen, Germany). Signal transmission/reception was achieved with a whole body volume resonator (72 mm i.d., Bruker Biospin) and a two-channel surface coil (RAPID Biomedical, Rimpar, Germany). Following acquisition of scout images, an automated field-mapping based shimming procedure was performed over a 4-mm coronal slice centred on the imaging volume of interest (located at −0.5 mm bregma), achieving a full width half maximum linewidth of 14.3 (±2.7 Hz). Images were then acquired using a diffusion-weighted flow-sensitive alternating inversion recovery (FAIR) sequence with a single coronal slice centred −0.5 mm from the bregma, single shot spin echo EPI readout and the following parameters: TR = 3500 ms, TI = 400 or 500 ms, TE = 33 ms, FOV = 30×30 mm^2, matrix size = 64×64, slice thickness = 2 mm, phase-encoding partial Fourier factor = 0.77, nominal b-value of MPGs = 20 s/mm^2, $\delta = 3$ ms, $\Delta = 6$ ms, slice selective inversion slab width = 8 mm. Images were acquired without MPGs (b0) and

then with the MPGs applied separately in the X, Y and Z directions. Taking into account the diffusion weighting of the imaging gradients, the effective *b*-values for the b0, X, Y and Z acquisitions were calculated to be 0.3, 21.6, 21.6 and 21.8 s/mm^2, respectively. In a single experiment, images were acquired for each MPG weighting and direction following both slice selective and global inversion, and this pattern was repeated 20 times. The TI was then changed from 500 ms to 400 ms (or vice versa) and the acquisition was performed again. This procedure was repeated 5 (four animals) or 4 times (one animal) for a total of 100 or 80 averages, respectively, at each MPG/ASL preparation/TI combination. Data acquisition was interleaved in this way to avoid differences due to systematic signal drift.

MRI data analysis

A simple model for brain MRI signal can be constructed as the sum of intra-vascular (IV) and extra-vascular (EV) contributions. Assuming that exchange between the IV and EV compartments is slow in comparison with the echo time, the total diffusion-weighted signal for a post-label delay of TI and labelling condition l may be written as

$$M^l(b_i, \mathrm{TI}) = M^l_{IV}(\mathrm{TI})e^{-b_i D^*_i} + M^l_{EV}(\mathrm{TI})e^{-b_i D_i}.$$

In this equation, D^*_i, D_i and b_i are the PDC, tissue apparent diffusion coefficient (ADC) and b-value, respectively, in direction $i \in \{X, Y, Z\}$. After subtracting the labelled and control acquisitions, the diffusion-weighted ASL signal is

$$\Delta M(b_i, \mathrm{TI}) = \Delta M_{IV}(\mathrm{TI})e^{-b_i D^*_i} + \Delta M_{EV}(\mathrm{TI})e^{-b_i D_i}.$$

where ΔM_{IV} and ΔM_{EV} represent the differences in the IV and EV contributions, respectively. The relatively short TIs employed in this work (400/500 ms) were chosen based on previous estimates of the arterial transit times (~200 ms[16,17]) and the mean exchange times (~400 ms[16,18]) of the rat cortex. Short TIs ensure that little of the labelled blood water exchanges into the extra-vascular tissue during the post-labelling delay, in which case it is expected that $\Delta M_{EV} \approx 0$, so that

$$\Delta M(b_i, \mathrm{TI}) \approx \Delta M_{IV}(\mathrm{TI})e^{-b_i D^*_i} \quad (1)$$

It follows that multidirectional diffusion-weighted ASL measurements at low b-value and short TI provide a means to estimate the PDC, and hence evaluate the anisotropy of the IV signal.

For each subject, images acquired following slice selective and global inversion were pair-wise subtracted to generate perfusion weighted images (ΔM). Maps of the PDC corresponding to application of the MPGs in the X, Y and Z directions were calculated by fitting the ΔM images to the simple mono-exponential model in equation (1). Five bilateral regions of interest (ROIs) were then manually drawn on the ΔM (b0) images from medial to lateral across the cortex (Figure 2(a)). Two additional ROIs were drawn within the anterior cerebral artery (ACA) and caudate putamen. For the ACA, the ROI was drawn on the perfusion weighted image acquired with MPGs applied in the Y direction, because the small arterial region is clearly identifiable in these images and is more difficult to accurately locate on the b0 images. Data from the ACA in subject 5 were not included as the ACA was not visible in the imaging slice. The average PDC in each direction was taken within each of the ROIs for each of the five rats.

To test hypothesis (1), a Spearman's non-parametric ranked correlation test was employed to examine whether there was a significant negative correlation between the ratio of D^*_Y/D^*_X across cortical ROIs 1–5. This was performed separately at TIs of 400 and 500 ms. The ranked test was employed using the cortical ROI number (1–5, from medial to lateral across the cortex) as the independent variable for the correlation analysis. Under the hypothesis that the principal direction of flow in the ACA is in the caudal-rostral (i.e. 'Z') direction, a paired t-test was employed to investigate whether D^*_Z was significantly greater than either D^*_X and D^*_Y within the ACA for each TI.

Within the cortex, the ratio D^*_Y/D^*_X was calculated and fit to a linear model against cortical ROI number (1–5) for TIs of 400 and 500 ms, respectively, for each rat. A paired t-test was used to investigate whether the gradient of D^*_Y/D^*_X against cortical ROI number was significantly different between TI = 400 ms and TI = 500 ms, across the five rats. This was performed to examine hypothesis (2), i.e. whether the extent of the directionality of the ΔM diffusion-weighted signal across the cortex is greater at TI = 400 ms relative to TI = 500 ms, across the five rats.

Finally, the ratio of D^*_Y/D^*_x was calculated on a pixel by pixel basis to generate spatial maps that convey the 2D directionality of the PDCs across the cortex (manually segmented). An anisotropic diffusion filter was applied to the spatial maps for image denoising.[19]

Results

Figure 1 shows representative control and ASL perfusion weighted (ΔM) images acquired with no diffusion weighting (b0) and with diffusion gradients (b-value = 20 s/mm^2) applied in three orthogonal

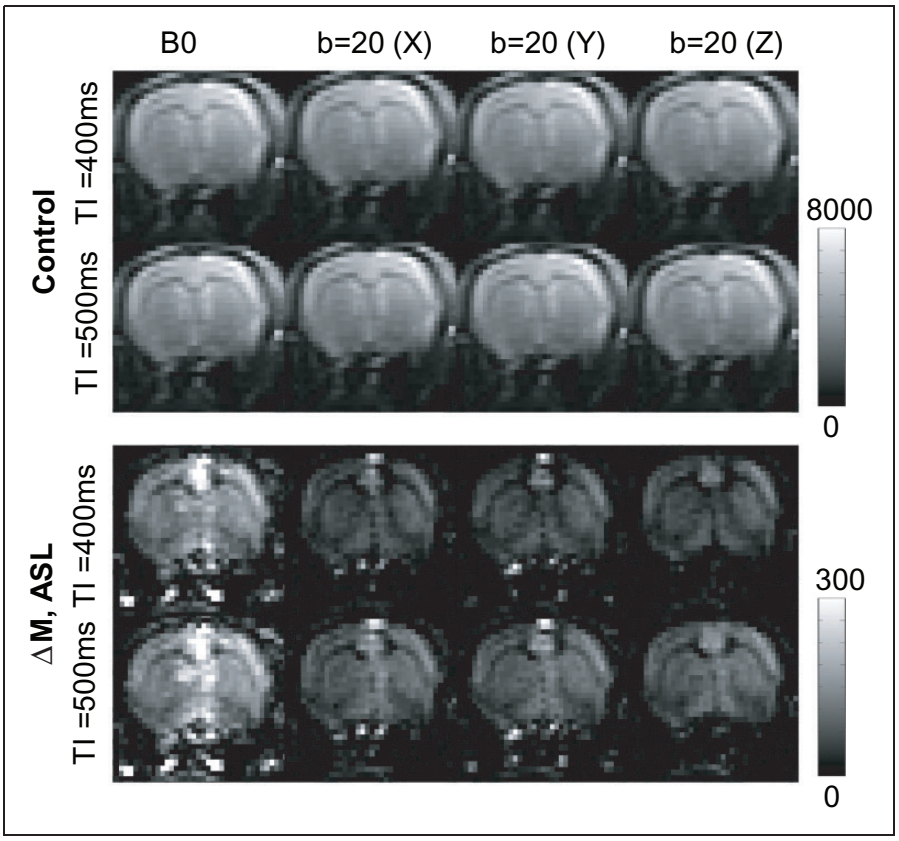

Figure 1. Representative control (rows 1–2) and ASL (rows 3–4) images (acquired following arterial spin labelling at TIs of 400 and 500 ms) with no diffusion weighting (B0) and with diffusion gradients applied in the X, Y and Z directions. The 'colour' bar shows the relative signal intensity (arbitrary units).

directions (X, Y, Z). As expected given the low *b*-value employed, the control images display minimal sensitivity to the applied MPGs. In contrast, the MPGs markedly attenuate the ΔM signal that principally derives from intravascular labelled blood water. Note the focal regions of ΔM hyper-intensity from large vessels outside the brain that are fully suppressed by application of the MPGs in the Z direction (parallel to the principal direction of flow (rostral-caudal)).

Figure 2 shows the estimated D* of the ΔM signal in the X, Y and Z directions within the ROIs across the cortex, ACA and caudate putamen (illustrated schematically in Figure 2(a)) at TIs of 400 and 500 ms. Overall, the calculated D* was approximately two orders of magnitude greater than that usually found for the ADC of rat brain grey matter[20] due to the dominant vascular origin of the ΔM signal at short TIs. Independent of pseudo-diffusion direction and ROI number, there was a significant decrease in cortical D* as TI increased from 400 to 500 ms (paired t-test, $p < 0.01$) as the source of the ASL signal shifts from the arterioles to the capillary bed at greater inflow time (Figure 2(c) and (d)). Visual inspection of Figure 2(c) and (d) shows that D* in all three orthogonal directions decreases then gradually increases from medial to lateral across the cortex. Although the precise reasons for the shape of these curves are unknown, this may reflect different vascular territories across the cortex and associated spatial heterogeneity of arterial transit time. Figure 3 shows the ratio D^*_Y/D^*_X across the cortex for $TI = 400$ ms and $TI = 500$ ms. At both TIs, D^*_Y/D^*_X gradually decreases from medial to lateral. A significant correlation was observed between the ratio D^*_Y/D^*_X and cortical ROI number 1–5 at both $TI = 400$ ms and $TI = 500$ ms (Spearman's ranked correlation coefficient, $p < 0.01$). This is consistent with the known orientation of the penetrating arterioles, which run perpendicular to the outer cortical surface (i.e. radially inwards (illustrated schematically in Figure 4(a))) and provides evidence to support hypothesis (1). In contrast, the mean estimates of D* within the caudate putamen are relatively similar at either TI (Figure 2(c) and (d)). This observation may reflect the vascular architecture of the caudate putamen, where there is a rapid transition to the capillary bed from the large arteries.[21] Within the ACA, D^*_Z was significantly greater than both D^*_X and D^*_Y at $TI = 400$ ms ($p = 0.013$ and 0.020, respectively) and at $TI = 500$ ms ($p = 0.002$ and 0.009, respectively (see Figure 2(b))).

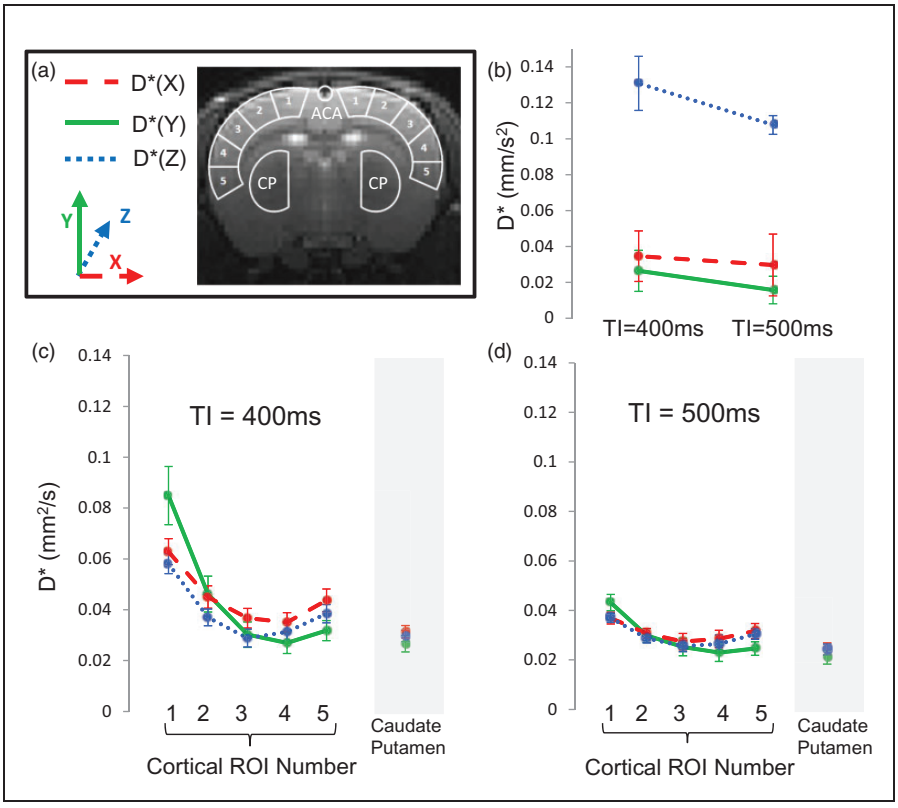

Figure 2. (a) T2 weighted spin echo image showing the anatomical location of the coronal imaging slice. Overlaid is a schematic representation of the ROIs from which mean D* estimates were taken: five bilateral cortical ROIs from medial to lateral; the caudate putamen (CP); anterior cerebral artery (ACA). (b) The estimated D* in X, Y and Z directions within the ACA at TIs of 500 ms and 400 ms. (c) The mean D* in X, Y and Z directions within cortical ROIs 1–5 and the CP at TI = 400 ms. (d) The mean D* in X, Y and Z directions within cortical ROIs 1–5 and the CP at TI = 500 ms. Error bars represent the standard error of the mean across the five rats.

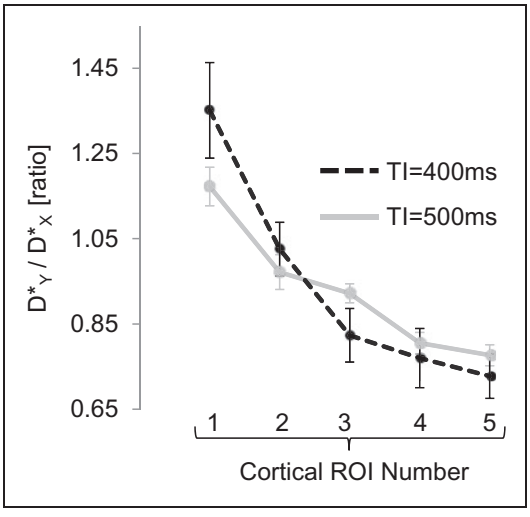

Figure 3. The ratio D*(Y)/D*(X) within the cortical ROIs (from medial to lateral) for TI = 400 ms and TI = 500 ms. Error bars represent standard error of the mean across the five rats.

This is concordant with the principal orientation of the ACA being caudal-rostral.

To examine the extent of the PDC directionality across the cortex, a simple linear fit was applied to the D^*_Y/D^*_X ratio (Figure 3) against cortical ROI number (1–5) for each rat. The gradient of the linear fit across the five rats was significantly greater at TI = 400 ms relative to TI = 500 ms ($p < 0.001$). This shows that the extent of the directionality of the PDCs across the cortex increases at shorter TI, which is consistent with the ASL signal being more weighted to the arterioles rather than the more isotropic capillary bed, and hence provides evidence in support of hypothesis (2). The D^*_Y/D^*_X ratio estimates from each rat and from each set of 20 averages (TI = 400 ms) are shown in Supplementary Figure 1 to give the interested reader an indication of the inter- and intra-animal reproducibility of these estimates.

Figure 4 shows spatial maps of the D^*_Y/D^*_X ratio across the cortex for a single rat at TIs of 400 and 500 ms. Visual inspection indicates a gradual transition of D^*_Y/D^*_X from the medial to lateral portion of the cortex across each hemisphere.

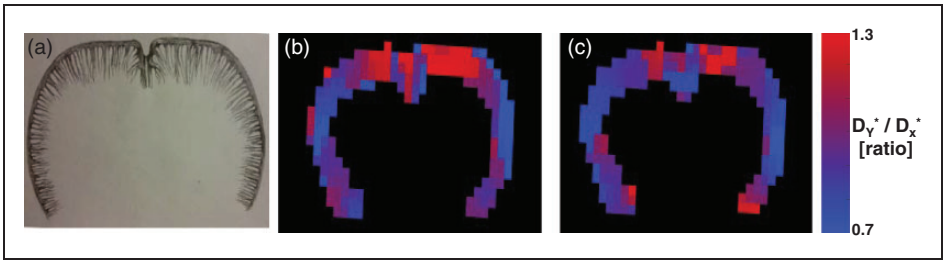

Figure 4. A schematic drawing illustrating the pattern of the penetrating arterioles in a coronal slice of the rat brain cortex (a). Spatial maps of D^*_Y/D^*_X across the cortex for a single rat at TI = 400 ms (b) and TI = 500 ms (c).

Discussion

In this study, we employed a hybrid ASL and multi-direction DWI sequence to image the dominant orientation of arterial micro-vascular flow patterns in the rat brain. Consistent, regionally dependent directionality of the estimated ΔM PDC (D*) was observed that followed the known morphometry of the penetrating arterioles in the cortex within a coronal slice[13,15] (Figures 2–4). Importantly, the extent of the ΔM PDC directionality across the cortex was significantly reduced at longer TI, reflecting transition of the labelled blood from the 'directionally ordered' penetrating vessels to the isotropic capillary bed (Figure 3). Thus, by modulating the TI of this sequence, it is possible to tune the measurements to different portions of the vascular tree. This novel approach is non-invasive and uses imaging principles (ASL and DWI) that are already established on clinical scanners, facilitating relative ease of translation to the human brain.

In conventional IVIM, images are typically acquired at multiple *b*-values and data are fitted to a bi-exponential model to estimate the 'high' and 'low' ADC components (attributed to the intra- and extra-vascular tissue space). The measured signal will be dominated by the extra-vascular compartment due to the low blood volume within the tissue (~5%[18]). In this work, we take a different approach and use ASL to isolate the measured signal from labelled blood water that has flowed into the brain. A key feature of this design is the use of a pulsed labelling scheme with a short TI, chosen to ensure that the ΔM signal is dominated by the intra-vascular compartment (on the arterial side of the vasculature). TIs of 400 and 500 ms were chosen based on the typical arterial transit time (~200 ms[16,17,22]) and exchange time (estimated by two previous studies to be 370 ms[16] and 400 ms[23]) in the rat cortex. In comparison with conventional IVIM, this avoids the necessity to perform multi-exponential fitting, a procedure that can be difficult because of its high sensitivity to noise.[24]

The diameter of penetrating arterioles in the rat cortex ranges from ~5 to 50 μm[1] and as such, cannot be individually spatially resolved *in vivo* with MRI due to limitations in SNR and spatial resolution. The technique presented in this work may provide a quantitative estimation of dominant arterial vessel orientation within an imaging voxel. The estimated PDCs represent a weighted average from labelled blood in the arterioles and capillaries. This is reflected in Figure 3, which illustrates that even in cortical ROIs 1 and 5 where the penetrating arterioles run most parallel to the diffusion gradients applied in the Y and X directions, respectively, the 2D directional bias (i.e. D^*_Y/D^*_X) of the estimated ΔM PDC in the coronal slice is only approximately 20–30%. Thus, the extent of the directional bias is less than traditional diffusion tensor imaging (DTI) of white matter where radial and axial diffusivity can differ by a factor of 2 or more. In future studies, careful modulation of TI and the applied diffusion weighting may enable extraction of directionally encoded PDCs originating from distinct vascular compartments (for example, using similar principles described in earlier work[18,23]).

Several previous studies have combined ASL and diffusion imaging techniques to investigate blood water delivery and exchange in the brain, with diffusion weighting applied in a single direction.[23,25–29] Another study used an intra-vascular perfluorocarbon contrast agent and ^{19}F NMR to examine the pseudo-diffusion properties of rat brain hemodynamics.[18] They observed a fast PDC ($D^* = 20–50 \times 10^{-3}$ mm^2/s) which they attributed to the arterial pool, in excellent agreement with the PDC (D*) values reported in this work (see Figure 2). A more recent study employed a velocity selective ASL scheme with multiple labelling directions to generate a 'perfusion tensor' in the brain.[30] However, in that work, the directional encoding was performed in the feeding vessels upstream of the eventual location of the labelled blood water during image acquisition (TI = 1.65 s). Consequently, there was a spatial mismatch between the site of directional encoding and the image, and therefore the tensor does not reflect

the local perfusion orientation. In contrast, the technique presented here has high spatial correspondence to micro-vascular orientation as directionality is encoded during the image acquisition phase rather than the labelling phase. An earlier conference abstract described a combined ASL and DTI approach to investigate the anisotropy of cerebral microvascular flow in the human brain.[31] However, they found no evidence for anisotropic cerebral microvascular flow, which may be a reflection of the variability of their measurements or the relatively long post-labelling delay time employed (resulting in exchange of the majority of the labelled blood water into the extra-vascular tissue space).

In this study, we chose to estimate the PDC of the ΔM signal in three directions, fewer than typically used in diffusion tensor imaging (DTI) studies.[32] The reason for this was to ensure that measurements for different diffusion encoding directions were closely interleaved in time to reduce the influence of MR signal drift on the precision of PDC estimation. In future applications, increased variety of applied diffusion gradient directions would permit improved accuracy of angular orientation measurement and allow the generation of an 'arterial micro-vascular flow tensor' from which quantitative properties such as the mean pseudo-diffusivity, fractional anisotropy and the principal eigenvector can be extracted. Furthermore, additional modelling of the directionally encoded ΔM PDC data could be performed to generate estimates of the micro-vascular volume fraction, the mean micro-flow velocity and the anisotropy of the vessels, using the models described in Karampinos et al.[10] The principal challenge of this technique is the small signal that is detected (see Figure 1) and in this work many signal averages were acquired to provide proof of principle data, resulting in relatively long imaging times ($\sim$45 min for each TI). However, with the continued progression of MRI scanner hardware (such as 'cryocoils'[33]) and sequence innovations (e.g. more efficient image readout schemes[34]), reliable detection of the ΔM PDC tensor may become feasible in clinically applicable imaging times.

In conclusion, we describe here a novel method to assess cerebral micro-vascular flow patterns using MRI. We provide evidence that the technique can detect the ordered architecture of the penetrating arterioles in the rat cortex. The ability to capture arteriole flow patterns may have significant value given recent evidence citing the role of micro-infarcts caused by occlusion of penetrating vessels in cognitive decline.[1,14] The method is non-invasive and may provide a useful translatable tool to improve understanding of perfusion and micro-vascular abnormalities in neurodegenerative disease.

Funding

The author(s) disclosed receipt of the following financial support for the research, authorship, and/or publication of this article: Brain/MINDS (Brain Mapping by Integrated Neurotechnologies for Disease Studies), MEXT Kakenhi (24300167). JW was supported by the Japanese Society for the Promotion of Science (JSPS). DLT was supported by the UCL Leonard Wolfson Experimental Neurology Centre (PR/ylr/18575).

Acknowledgements

We would like to thank Nobuhiro Nitta, Sayaka Shibata and Yoshikazu Ozawa for their excellent technical contributions to this project. We would also like to thank Daisuke Kokuryo (Kobe University) for his support to the project. The authors would like to thank Jenifer Crouch for the schematic drawing of the penetrating arterioles in the rat brain cortex (http://www.jennifercrouch.com/).

Declaration of conflicting interests

The author(s) declared no potential conflicts of interest with respect to the research, authorship, and/or publication of this article.

Authors' contributions

JAW performed the experiments, analysed the data and wrote the manuscript. DLT helped conceive the technique, provided intellectual guidance throughout and edited the manuscript. JK helped program the MRI sequence, helped analyse the data, edited the manuscript and provided intellectual guidance throughout. TS and IA directed and facilitated the research, optimised the MRI and animal related apparatus and edited the manuscript.

Supplementary material

Supplementary material for this paper can be found at http://jcbfm.sagepub.com/content/by/supplemental-data

References

1. Shih AY, Blinder P, Tsai PS, et al. The smallest stroke: occlusion of one penetrating vessel leads to infarction and a cognitive deficit. *Nat Neurosci* 2013; 16: 55–63.
2. Ostergaard L, Aamand R, Gutierrez-Jimenez E, et al. The capillary dysfunction hypothesis of Alzheimer's disease. *Neurobiol Aging* 2013; 34: 1018–1031.
3. de la Torre JC. The vascular hypothesis of Alzheimer's disease: bench to bedside and beyond. *Neurodegener Dis* 2010; 7: 116–121.
4. Jones D. *Diffusion MRI: Theory, methods and applications*, 1st ed. Oxford: Oxford University Press, 2011.
5. Moseley ME, Cohen Y, Kucharczyk J, et al. Diffusion-weighted MR imaging of anisotropic water diffusion in cat central nervous system. *Radiology* 1990; 176: 439–445.
6. Beaulieu C. The basis of anisotropic water diffusion in the nervous system - a technical review. *NMR Biomed* 2002; 15: 435–455.

7. Le Bihan D. Intravoxel incoherent motion perfusion MR imaging: a wake-up call. *Radiology* 2008; 249: 748–752.
8. Henkelman RM. Does IVIM measure classical perfusion? *Magn Reson Med* 1990; 16: 470–475.
9. Federau C, Maeder P, O'Brien K, et al. Quantitative measurement of brain perfusion with intravoxel incoherent motion MR imaging. *Radiology* 2012; 265: 874–881.
10. Karampinos DC, King KF, Sutton BP, et al. Intravoxel partially coherent motion technique: characterization of the anisotropy of skeletal muscle microvasculature. *J Magn Reson Imag* 2010; 31: 942–953.
11. Abdullah OM, Gomez AD, Merchant S, et al. Orientation dependence of microcirculation-induced diffusion signal in anisotropic tissues. *Magn Reson Med*. Epub ahead of print 29 October 2015. DOI: 10.1002/mrm.25980.
12. Notohamiprodjo M, Chandarana H, Mikheev A, et al. Combined intravoxel incoherent motion and diffusion tensor imaging of renal diffusion and flow anisotropy. *Magn Reson Med* 2015; 73: 1526–1532.
13. Paxinos G. *The rat nervous system*. 3rd ed. Amsterdam: Elsevier, 2004.
14. Blinder P, Tsai PS, Kaufhold JP, et al. The cortical angiome: an interconnected vascular network with noncolumnar patterns of blood flow. *Nat Neurosci* 2013; 16: 889–897.
15. Dacey RG Jr and Duling BR. A study of rat intracerebral arterioles: methods, morphology, and reactivity. *Am J Physiol* 1982; 243: H598–H606.
16. Wells JA, Siow B, Lythgoe MF, et al. Measuring biexponential transverse relaxation of the ASL signal at 9.4 T to estimate arterial oxygen saturation and the time of exchange of labeled blood water into cortical brain tissue. *J Cereb Blood Flow Metab* 2013; 33: 215–224.
17. Wells JA, Lythgoe MF, Gadian DG, et al. In vivo Hadamard encoded continuous arterial spin labeling (H-CASL). *Magn Reson Med* 2010; 63: 1111–1118.
18. Duong TQ and Kim SG. In vivo MR measurements of regional arterial and venous blood volume fractions in intact rat brain. *Magn Reson Med* 2000; 43: 393–402.
19. Wells JA, Thomas DL, King MD, et al. Reduction of errors in ASL cerebral perfusion and arterial transit time maps using image de-noising. *Magn Reson Med* 2010; 64: 715–724.
20. Thomas DL, Lythgoe MF, Pell GS, et al. The measurement of diffusion and perfusion in biological systems using magnetic resonance imaging. *Phys Med Biol* 2000; 45: R97–R138.
21. Rieke GK, Bowers DE Jr and Penn P. Vascular supply pattern to rat caudatoputamen and globus pallidus: scanning electronmicroscopic study of vascular endocasts of stroke-prone vessels. *Stroke* 1981; 12: 840–847.
22. Thomas DL, Lythgoe MF, van der Weerd L, et al. Regional variation of cerebral blood flow and arterial transit time in the normal and hypoperfused rat brain measured using continuous arterial spin labeling MRI. *J Cerebr Blood Flow Metab* 2006; 26: 274–282.
23. Kim T and Kim SG. Quantification of cerebral arterial blood volume using arterial spin labeling with intravoxel incoherent motion-sensitive gradients. *Magn Reson Med* 2006; 55: 1047–1057.
24. King MD, van Bruggen N, Busza AL, et al. Perfusion and diffusion MR imaging. *Magn Reson Med* 1992; 24: 288–301.
25. Silva AC, Williams DS and Koretsky AP. Evidence for the exchange of arterial spin-labeled water with tissue water in rat brain from diffusion-sensitized measurements of perfusion. *Magn Reson Med* 1997; 38: 232–237.
26. Wang J, Alsop DC, Song HK, et al. Arterial transit time imaging with flow encoding arterial spin tagging (FEAST). *Magn Reson Med* 2003; 50: 599–607.
27. Wang J, Fernandez-Seara MA, Wang S, et al. When perfusion meets diffusion: in vivo measurement of water permeability in human brain. *J Cerebr Blood Flow Metab* 2007; 27: 839–849.
28. Hales PW and Clark CA. Combined arterial spin labeling and diffusion-weighted imaging for noninvasive estimation of capillary volume fraction and permeability-surface product in the human brain. *J Cerebr Blood Flow Metab* 2013; 33: 67–75.
29. Wells JA, Lythgoe MF, Choy M, et al. Characterizing the origin of the arterial spin labelling signal in MRI using a multiecho acquisition approach. *J Cereb Blood Flow Metab* 2009; 29: 1836–1845.
30. Frank LR, Lu K and Wong EC. Perfusion tensor imaging. *Magn Reson Med* 2008; 60: 1284–1291.
31. Priya AK, Yan L and Wang DJ. Is cerebral microvascular flow anisotropic - preliminary evidence from multidirectional diffusion weighted perfusion MRI. In: *Proceedings of international society for magnetic resonance in medicine*, Montreal, Canada, 2011.
32. Jones DK and Leemans A. Diffusion tensor imaging. *Meth Mol Biol* 2011; 711: 127–144.
33. Radzwill NI, Haueisen R, Marek D, et al. Benefits of cryogenic coils for routine in-vivo mouse brain imaging and spectroscopy at 9.4 T. In: *Proceedings of international society for magnetic resonance in medicine*, Berlin, Germany, 2007.
34. Vidorreta M, Balteau E, Wang Z, et al. Evaluation of segmented 3D acquisition schemes for whole-brain high-resolution arterial spin labeling at 3 T. *NMR Biomed* 2014; 27: 1387–1396.